

Iwr1 Directs RNA Polymerase II Nuclear Import

Elmar Czeko,¹ Martin Seizl,¹ Christian Augsberger,¹ Thorsten Mielke,² and Patrick Cramer^{1,*}¹Gene Center and Department of Biochemistry, Center for Integrated Protein Science Munich (CIPSM), Ludwig-Maximilians-Universität München, Feodor-Lynen-Strasse 25, 81377 Munich, Germany²Ultrastrukturnetzwerk, Max Planck Institute for Molecular Genetics, Ihnestrasse 63-73, 14195 Berlin, Germany*Correspondence: cramer@genzentrum.lmu.de

DOI 10.1016/j.molcel.2011.02.033

SUMMARY

RNA polymerase (Pol) II transcribes protein-coding genes in the nucleus of eukaryotic cells and consists of 12 polypeptide subunits. It is unknown how Pol II is imported into the nucleus. Here we show that Pol II nuclear import requires the protein Iwr1 and provide evidence for cyclic Iwr1 function. Iwr1 binds Pol II in the active center cleft between the two largest subunits, maybe facilitating or sensing complete Pol II assembly in the cytoplasm. Iwr1 then uses an N-terminal bipartite nuclear localization signal that is recognized by karyopherin α to direct Pol II nuclear import. In the nucleus, Iwr1 is displaced from Pol II by transcription initiation factors and nucleic acids, enabling its export and recycling. Iwr1 function is Pol II specific, transcription independent, and apparently conserved from yeast to human.

INTRODUCTION

Pol II is the conserved 12-subunit enzyme that transcribes mRNA from protein-coding genes in the nucleus of eukaryotic cells. Whereas the structure and function of Pol II have been extensively studied (Cramer et al., 2008), its biogenesis is not well understood. Only recently, two proteomic studies investigated the assembly of Pol II from its subunits (Boulon et al., 2010; Forget et al., 2010). In one study, depletion of any Pol II subunit in human cells resulted in cytoplasmic accumulation of the largest subunit, Rpb1, indicating that Pol II assembly takes place in the cytoplasm and precedes nuclear import (Boulon et al., 2010). Cytoplasmic Rpb1 accumulation was also observed after treatment of cells with leptomycin B, a nuclear export inhibitor, suggesting nuclear trapping of a factor that directs Pol II import. Unassembled Rpb1 was reported to bind the HSP90 cochaperone hSpagh (RPAP3), the R2TP/Prefoldin complex, and RPAP4/GPN1, which was also bound by an assembly intermediate consisting of Rpb2, Rpb3, and Rpb10–12. In a second study, knock-down of RPAP4/GPN1 led to cellular delocalization of Rpb1 and Rpb2 (Forget et al., 2010). These studies suggest two major assembly intermediates of Pol II: one containing Rpb1, and one containing Rpb2 together with the Rpb3/10/11 subcomplex, consistent with biochemical (Kimura et al., 1997) and structural data (Cramer et al., 2000) on Pol II subunit interactions. Thus,

some insights into the cellular assembly of Pol II were obtained, but the mechanism of how Pol II is imported into the nucleus remains elusive. Here we show that the conserved protein Iwr1 specifically binds Pol II between Rpb1 and Rpb2 and directs its nuclear import.

RESULTS

Since Pol II subunit sequences lack a known nuclear localization signal (NLS), Pol II likely binds an additional NLS-containing factor that mediates nuclear import. Analysis of the protein interactome in the yeast *Saccharomyces cerevisiae* showed that Pol II subunits copurify with the protein YDL115c (Gavin et al., 2002; Krogan et al., 2006), which was later renamed Iwr1, for “interacts with RNA polymerase II 1” (Pagé et al., 2003). Inspection and bioinformatic analysis (Kosugi et al., 2009) of the Iwr1 sequence revealed a putative bipartite NLS in the N-terminal protein region (Figure 1A). This sequence encodes a functional NLS, as it could target a 150 kDa heterologous reporter protein to the nucleus (Figure S1A).

To test whether Iwr1 may import Pol II into the nucleus, we constructed a yeast strain carrying a fusion of the genes encoding the Pol II subunit Rpb3 and the green fluorescent protein variant EGFP (Experimental Procedures). In growing cells from this strain, fluorescence was restricted to the nucleus, indicating that Pol II was localized in the nucleus as expected (Figure 1C). However, in a strain that additionally contained a deletion of the gene encoding Iwr1 (Δ Iwr1), Rpb3 was localized in the cytoplasm (Figure 1C). Since Rpb3 is a component of the Rpb2-containing assembly intermediate, we also investigated localization of Rpb1 in the Δ Iwr1 background and found it is also localized to the cytoplasm (Figure 1D). These results indicate that the entire Pol II enzyme is mislocalized. Nuclear localization of Pol II could, however, be rescued by transformation of a plasmid expressing Iwr1 from its natural promoter (Figure 1C). Rescue depended on the NLS of Iwr1, as it was not achieved with Iwr1 variants that lacked the NLS or carried mutations in the two NLS sites (Figures 1A, 1C, and S1B). Since expression of the human Iwr1 homolog partially restored Pol II mislocalization and cellular shape (Figure 1C), Iwr1 function is apparently conserved among eukaryotes.

To investigate whether Pol II binds directly to Iwr1 in vitro, we incubated pure yeast Pol II with recombinant Iwr1 and subjected the mixture to size-exclusion chromatography. A stoichiometric Pol II-Iwr1 complex was obtained (Figures 2C and 2D), indicating a direct interaction that did not require additional factors or Iwr1

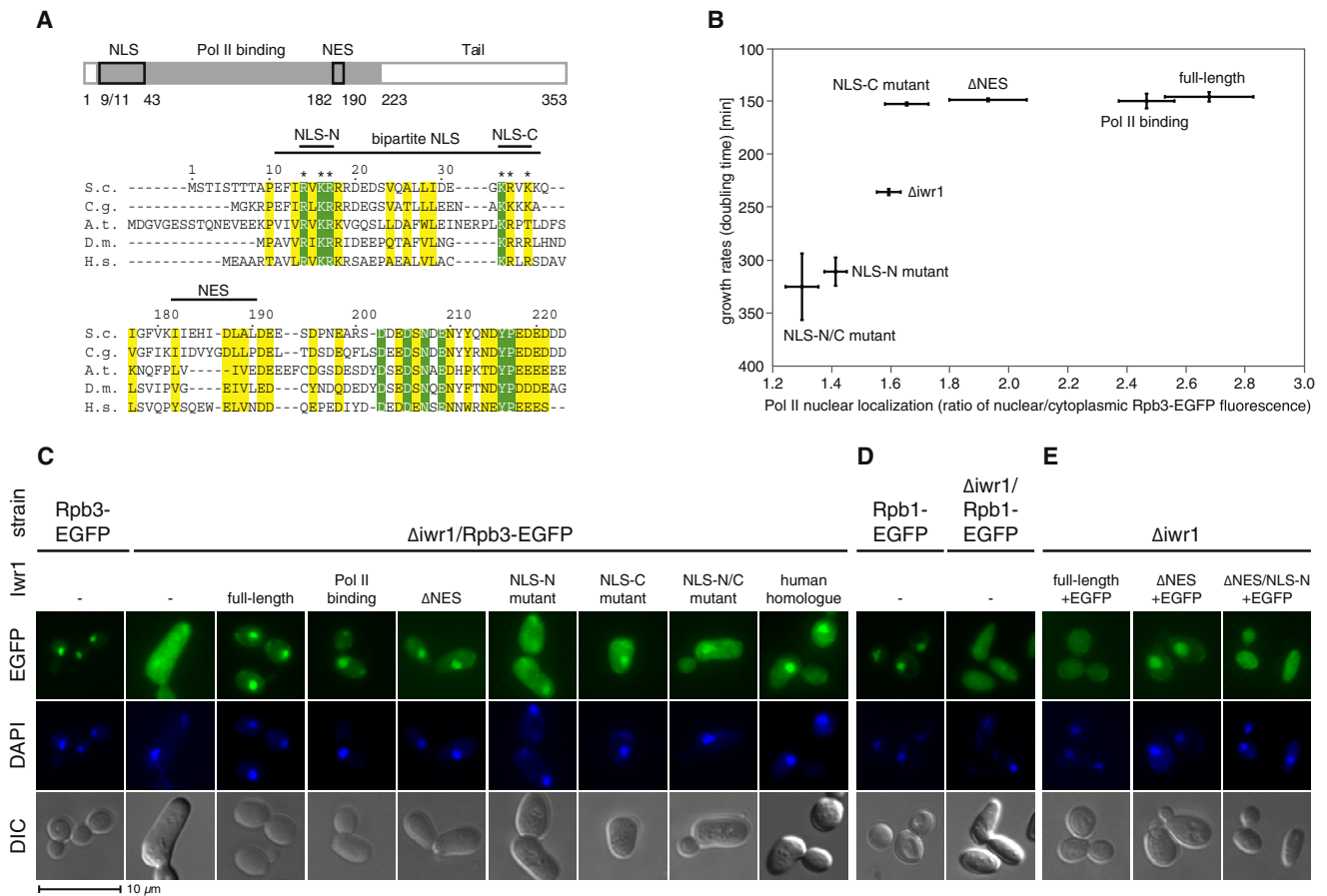


Figure 1. *lwr1* Directs Pol II Nuclear Import

(A) Schematic representation of yeast (*S.c.*), *lwr1*, and amino acid sequence conservation. The Pol II-binding region is indicated in gray, boxes delineate NLS and NES sequences. Invariant residues are highlighted in green, residues with $\geq 80\%$ conservation in yellow. Asterisks indicate mutations to alanine in the mutant variants. S.c., *Saccharomyces cerevisiae* (Q07532); C.g., *Candida glabrata* (Q6FR91); A.t., *Arabidopsis thaliana* (NM_128581); D.m., *Drosophila melanogaster* (NP_524940); H.s., *Homo sapiens* (BC013778); NCBI accession numbers are indicated in brackets.

(B) Correlation of cellular growth rates and Pol II nuclear localization in $\Delta iwr1$ /Rpb3-EGFP cells expressing the indicated *lwr1* variants. Mean ratio of quantified nuclear/cytoplasmic Rpb3-EGFP fluorescence ($n \geq 10$ cells, \pm SEM) plotted against growth rates (triplicates from three independent cultures, \pm SEM).

(C–E) Localization of Rpb3- (C), Rpb1- (D), and *lwr1*-EGFP (E) in wild-type and $\Delta iwr1$ cells expressing the indicated *lwr1* variants (–, empty plasmid). Nuclear staining with 4',6-diamidino-2-phenylindole (DAPI). DIC, differential interference contrast. See also Figure S1.

phosphorylation (Albuquerque et al., 2008). Recombinant *lwr1* variants with NLS mutations bound Pol II normally (Figure S2A), showing that the failure of such variants to rescue Pol II nuclear localization (Figures 1B and 1C) was not due to impaired Pol II binding, but due to impaired NLS function. Binding studies with truncated *lwr1* variants delineated a minimal Pol II-binding region in *lwr1* (Figures 1A and S2B) that comprised the NLS and sufficed to rescue Pol II localization (Figures 1B and 1C and S1B).

We elucidated the architecture of the Pol II-*lwr1* complex by cryo-electron microscopy (cryo-EM). In negative stain, the Pol II-*lwr1* complex formed single particles of the expected size (Figure 2B). Cryo-EM images were collected, and an electron density map at 21 Å resolution was reconstructed from 25,206 particles (Figures 2A and S2F). A difference density map between the cryo-EM reconstruction and the free Pol II crystal structure revealed a major density in the Pol II active center cleft (Cramer et al., 2001) that was attributed to *lwr1* (Figure 2A). The difference

density volume does not fully account for the *lwr1* molecular weight, suggesting that parts of *lwr1* remain flexible in the Pol II-*lwr1* complex, as required to keep the NLS accessible to the import machinery. Consistent with this model, the Pol II-*lwr1* complex bound the karyopherin α variant GST-Kap60 Δ 73 in vitro (Figures S2G and S2H). Binding of *lwr1* in the cleft between the two large Pol II subunits suggests that *lwr1* only binds Pol II that is completely assembled, preventing nuclear import of nonfunctional assembly intermediates.

The cryo-EM results predicted that nucleic acids that interact with the active center cleft compete with *lwr1* for Pol II binding. Consistent with this prediction, a DNA-RNA scaffold and an RNA inhibitor that both bind in the cleft (Kettenberger et al., 2006) displaced *lwr1* from a Pol II-*lwr1* complex in vitro (Figures 2D and S2C). Thus, *lwr1* must liberate the cleft for nucleic acid binding, arguing against a suggested role of *lwr1* in transcription (Peiró-Chova and Estruch, 2009). Indeed, recombinant *lwr1* did

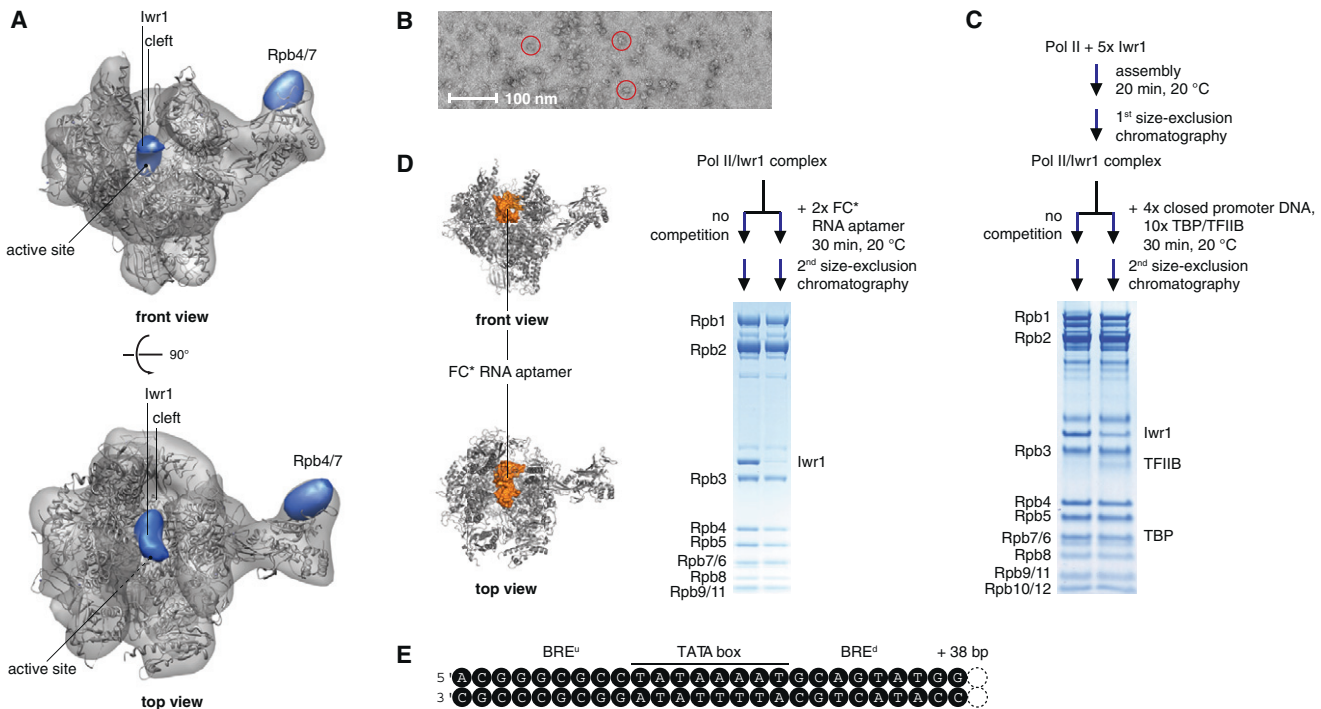


Figure 2. Iwr1 Binds Pol II in the Active Center Cleft

(A) Cryo-EM map of the Pol II-Iwr1 complex at 21 Å resolution (gray). The difference density between this map and a Pol II crystal structure (PDB: 1WCM), both filtered to 25 Å, is in blue. A difference density calculated with a free Pol II cryo-EM reconstruction is consistent, albeit noisier (data not shown). Pol II views and regions are as previously defined (Cramer et al., 2001). Figures were prepared with UCSF Chimera (<http://www.cgl.ucsf.edu/chimera>). (B) Electron micrograph of Pol II-Iwr1 complexes negatively stained with uranyl acetate. Red circles indicate distinct Pol II-Iwr1 complexes. (C and D) Coomassie-stained SDS-PAGE of the Pol II-Iwr1 complex after size-exclusion chromatography, before (left) and after (right) competition with either promoter DNA-TBP-TFIIB complex (C) or the RNA aptamer FC* RNA aptamer (Kettenberger et al., 2006) (D). The identity of the bands was confirmed by mass spectrometry. FC* as located in the X-ray structure is in orange (PDB: 2B63). Figures were prepared with PyMOL (Schrödinger, LLC, San Diego, CA) (D). (E) Sequence of the closed promoter DNA used in (C). BRE^u, upstream/downstream TFIIB recognition element. See also Figure S2.

not influence RNA elongation by Pol II in vitro (data not shown). Iwr1 was also not required for promoter-dependent transcription, as a nuclear extract from $\Delta iwr1$ cells supported transcription in vitro (Figures 3A and 3B). Transcription was even quenched upon addition of recombinant Iwr1, likely by the formation of inactive Pol II-Iwr1 complexes (Figure 3B). Further, the gene expression profile of the $\Delta iwr1$ strain was not related to any profile of 263 transcription factor gene deletion strains (Hu et al., 2007; Reimand et al., 2010) (Figure 3C). Instead, a lack of Iwr1 led to pleiotropic effects on gene expression in vivo (Tables S1 and S2). A total of 794 mRNA levels were significantly changed, with 60% being decreased, generally consistent with previous data (Bianchi et al., 2001) and likely accounting for an altered cellular shape (Figures 1C–1E).

These results argued against a role of Iwr1 in transcription, but for a general role of Iwr1 in Pol II nuclear import. To further support this, we compared $\Delta iwr1$ strains expressing different Iwr1 variants for their growth rates and levels of Pol II nuclear localization (Figure 1B). Strains expressing Iwr1 variants that partially rescued Pol II localization generally grew faster than strains expressing variants that did not rescue Pol II localization, and the N-terminal part of the bipartite NLS was critical for both. Thus, Pol II nuclear import is a key function of Iwr1 in vivo.

To test whether Iwr1 may also regulate the expression of Pol II subunits and, thus, cellular levels of Pol II, we measured the protein level of the Pol II-specific subunit Rpb3, which is limiting in Pol II complex formation (Kimura et al., 2001). Rpb3 levels were unaltered in cells lacking Iwr1 (Figure S1C), indicating that Pol II concentrations are unaltered in the knockout cells and that Pol II mislocalization is not a result of excess Pol II accumulation in the cytoplasm. Levels of the Pol II subunit Rpb1 were, however, higher in cells lacking Iwr1 (Figure S1C). This was not due to increased Rpb1 mRNA levels, as measured by transcriptomics (Figure 3C), but rather a consequence of Rpb1 protein stabilization. Indeed, the Rpb1 protein half-life was increased (Figure S1D), indicating reduced Rpb1 degradation, which occurs cotranscriptionally (Somesh et al., 2005, 2007).

We next asked how Iwr1 is recycled after the Pol II-Iwr1 complex enters the nucleus. The location of Iwr1 in the Pol II cleft suggested that Iwr1 is displaced when Pol II assembles with transcription initiation factors on promoter DNA. Indeed, the initiation factor TFIIB, which contains regions that bind in the cleft (Kostrewa et al., 2009), partially displaced Iwr1 from Pol II in vitro (Figure S2D). Iwr1 was also partially displaced from Pol II upon addition of a minimal promoter DNA complex containing TFIIB and the TATA box-binding protein TBP (Figure 2C). Iwr1

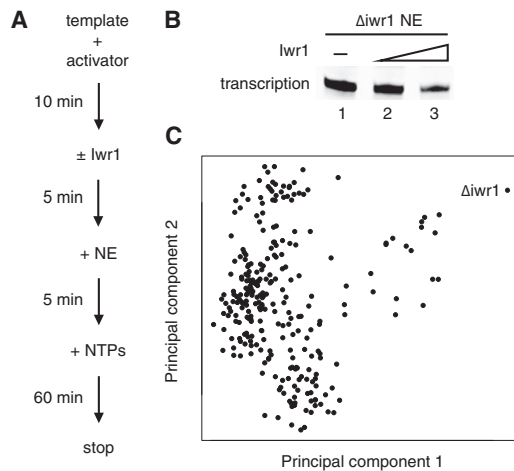


Figure 3. *lwr1* Is Not a Transcription Factor

(A) Schematic representation of the promoter-dependent transcription assay. NE, nuclear extract.

(B) Promoter-dependent transcription assay with nuclear extract from $\Delta lwr1$ cells. Bands indicate the transcriptional signal. In lanes 2 and 3, 1 and 10 pmol, respectively, of recombinant *lwr1* were added to the reaction.

(C) The $\Delta lwr1$ gene expression profile does not resemble any known transcription factor knockout profile. The correlation between the profiles (relative to wild-type) was calculated. The first two principal components of the correlation matrix are plotted. $\Delta lwr1$ is indicated as a red dot. See also Tables S1 and S2.

displacement may liberate a nuclear export signal (NES) that is present in *lwr1* (Peiró-Chova and Estruch, 2009). The NES is required for full restoration of Pol II localization in vivo (Figure 1B). Consistent with these results, fluorescently labeled *lwr1* is distributed over the cell, but is trapped in the nucleus upon NES deletion (Figures 1A and 1E). Combining the NES deletion with NLS mutations abolished nuclear trapping of *lwr1*, indicating that nuclear import of *lwr1* is solely directed by its own NLS (Figure 1E). These results indicate that the nuclear Pol II-*lwr1* complex disassembles when Pol II forms a promoter complex for transcription and that liberated *lwr1* is recycled by nuclear export, facilitated by its NES.

Finally, we investigated whether *lwr1* also directs import of eukaryotic Pol I and Pol III. We constructed yeast strains carrying an EGFP fusion of the gene encoding Rpa190 or C160, the largest subunits in Pol I and Pol III, respectively (Figure S1E). Nuclear localization of the Pol I and Pol III subunits was essentially unchanged in the $\Delta lwr1$ strain. Consistently, we did not observe binding of *lwr1* to purified Pol I or Pol III in vitro (data not shown). These results establish *lwr1* as a Pol II-specific nuclear import adaptor that does not import Pol I and Pol III. However, in plant cells, *lwr1* may import Pol IV and Pol V, two plant-specific, Pol II-related enzymes (Ream et al., 2009), because *lwr1* is required for Pol IV/V-dependent processes in *Arabidopsis* (He et al., 2009; Kanno et al., 2010).

DISCUSSION

Our results can be explained with a cyclic model for *lwr1* function in Pol II nuclear import (Figure 4). *lwr1* binds Pol II that is assem-

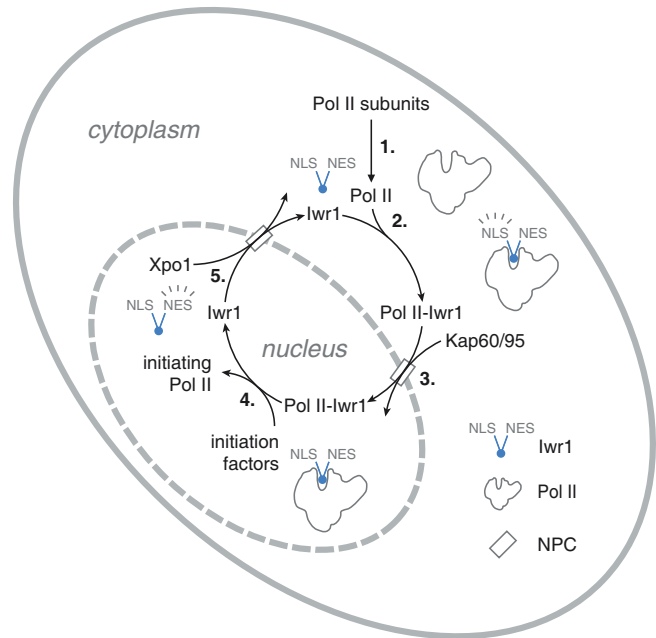


Figure 4. Cyclic Model for *lwr1*-Directed Pol II Nuclear Import

Pol II assembles from its subunits in the cytoplasm (1). *lwr1* senses complete assembly by binding in the Pol II cleft (2). The *lwr1* NLS directs Pol II import through the nuclear pore complex via Kap60/95 (NPC, 3). Assembly of Pol II with initiation factors on promoter DNA releases *lwr1* (4). The *lwr1* NES facilitates nuclear export via Xpo1, completing the cycle (5).

bled in the cytoplasm. *lwr1* then uses its bipartite NLS to direct Pol II nuclear import. *lwr1* binding between the large Pol II subunits may sense complete Pol II assembly and limit nuclear import to functional Pol II. In the nucleus, *lwr1* is displaced from the Pol II active center cleft during formation of the transcription initiation complex on promoter DNA. Liberated *lwr1* is then exported from the nucleus with the help of its NES. Finally, *lwr1* can bind and import another Pol II complex into the nucleus, closing the cycle. Cyclic *lwr1* function is apparently conserved throughout eukaryotes, since the human *lwr1* homolog can partially substitute the yeast protein in cells. Functional conservation is also suggested by a conservation of amino acid sequence in the functionally relevant Pol II-binding region of 39% (23% identity) and 31% overall (20% identity).

Together with two recent reports (Boulon et al., 2010; Forget et al., 2010), our results provide a starting point for analyzing the mechanisms of RNA polymerase biogenesis and cellular localization. Our data are consistent with Pol II assembly in the cytoplasm and Pol II degradation in the nucleus and also generally with recent observations (Boulon et al., 2010; Forget et al., 2010). One published observation seems inconsistent, namely that small Pol II subunits are not delocalized in the cell when the presumed assembly factor RPAP4/GPN1 is depleted, which led to the suggestion that Pol II assembly may be nuclear (Forget et al., 2010). However, there are alternative explanations for this observation, including a role for the poorly characterized factor RPAP4/GPN1 that is different from the one assumed and a possible rapid degradation of nonassembled small Pol II subunits.

Finally, alternative, less efficient pathways for Pol II nuclear import may exist. The $\Delta iwr1$ strain is very sick, but viable, and thus a fraction of Pol II must be imported into the nucleus in an *lwr1*-independent manner. Such inefficient, fractional Pol II import may be mediated by any Pol II-binding factor that contains an NLS, such as the general transcription factors TFIIB and TFIIF (Hodges et al., 2005; Süel and Chook, 2009). This is consistent with the observation that strains expressing *lwr1* variants that contain mutations in NLS-N grow more slowly than strains that do not express *lwr1* at all (Figure 1B). In these cases, functionally deficient *lwr1* binds Pol II (Figure S2A) and likely blocks binding of alternative NLS-containing factors. The observation that *lwr1* is Pol II specific may indicate that RNA polymerase biogenesis and nuclear localization provide an additional level of genomic regulation that can set global expression levels, as suggested recently (Zhurinsky et al., 2010).

EXPERIMENTAL PROCEDURES

Strains and Constructs

The generation of strains and constructs is described in Supplemental Information.

Growth Analysis and Microscopy

For growth curves in SC-Ura medium of Rpb3-EGFP/ $\Delta iwr1$ cells transformed with *lwr1* rescue constructs, triplicate cultures were inoculated from an overnight culture at an optical density at 600 nm (OD_{600}) of 0.1 and grown for up to 9 hr at 30°C. For each culture, doubling times were calculated based on four OD_{600} measurements during the exponential growth phase. For microscopic analysis, Rpb3-EGFP, Rpb3-EGFP/ $\Delta iwr1$, $\Delta iwr1$, or wild-type cells transformed with different *lwr1* rescue or NLS reporter constructs were grown to an OD_{600} of 0.8 in SC-Ura or -Leu medium. For Rpb1-EGFP, Rpb4-EGFP, Rpa190-EGFP, and C160-EGFP cells with or without *iwr1* deletion, YPD medium was used. Cells were harvested in exponential phase, fixed with 5% (w/v) paraformaldehyde, transferred to glass slides treated with 0.02% (w/v) poly-L-Lys (Sigma-Aldrich, Hamburg, Germany), stained with 1 μ g/ml DAPI (4',6-diamidino-2-phenylindole) in PBS for 10 min, and washed three times with PBS. Imaging was performed with a Leica AF6000 fluorescence microscope at 100 \times magnification and the Leica LAS AF Software (Wetzlar, Germany). Quantification of nuclear and cytoplasmic fluorescence was done with ImageJ (<http://rsbweb.nih.gov/ij/>). For EGFP images, linear contrast adjustment was used. For DAPI images, nonlinear contrast adjustment was used in some cases to facilitate the identification of the nucleus.

Pol II-Iwr1 Complex Preparation

Endogenous *S. cerevisiae* Pol II core and recombinant Rpb4/7 were purified as described (Sydow et al., 2009). Full-length *lwr1* and truncation variants were purified as described in Supplemental Information. Pol II core, Rpb4/7, and *lwr1* were mixed in a 1:5:5 molar ratio, incubated at 20°C for 20 min, and applied to a Superose 6 size-exclusion column (GE Healthcare, Munich, Germany). The eluted Pol II-Iwr1 complex was concentrated and subjected to cryo-EM analysis and single particle reconstruction as described in Supplemental Information.

Complex Formation and Transcription Assays

For competition experiments, the promoter scaffold was annealed as described (Damsma et al., 2007), and TBP and TFIIB were purified as described (Kostrewa et al., 2009). GST-Kap60 Δ 73 was purified as described (Cook et al., 2005). Species to be assembled were added in different stoichiometric ratios and incubated as indicated (Figures 2C, 2D, S2G, and S2H), and this was followed by size-exclusion chromatography and analysis of peak fractions by TCA precipitation, SDS-PAGE, and mass spectrometry. Yeast nuclear extracts were prepared from 3 l of culture as described (<http://www.fhcr.org/labs/hahn>).

In vitro transcription and primer extension was as reported (Larivière et al., 2008; Ranish and Hahn, 1991).

Gene Expression Analysis

The $\Delta iwr1$ strain and an isogenic wild-type strain were grown in YPD medium with 2% (w/v) glucose. Microarray analysis was performed as described (Koschubs et al., 2009). Classification of significantly differentially expressed genes was carried out according to the Super GO-Slim Mapper (<http://www.yeastgenome.org>). Comparison of the IWR1 profile with those of transcription factors was done using the reanalysis (Reimand et al., 2010) of a yeast knockout compendium (Hu et al., 2007). Pairwise Pearson correlations of the fold expression relative to wild-type were calculated between all profiles. The first two principal components of the resulting correlation matrix were visualized (Figure 3C).

Immunoblots and Rpb1 Half-Life Determination

Yeast cells were grown to exponential phase and lysed in alkaline conditions (1.85 M NaOH, 7.5% [v/v] β -mercaptoethanol) on ice for 20 min with intermittent vortexing, followed by protein precipitation on ice for 20 min with 25% (w/v, final) trichloroacetic acid. Precipitate was pelleted and redissolved in SDS loading buffer and run on an SDS-PAGE. Immunoblots were performed essentially as previously described (Knop et al., 1996), using the antibodies α -Pgk (mouse, 1:20,000; Invitrogen, Carlsbad, CA), α -Rpb1/8WG16 (mouse, 1:500; Covance, Princeton, NJ), α -Rpb3 (mouse, 1:2000; Neoclone, Madison, WI), and α -mouse HRP-coupled (goat, 1:3000; Bio-Rad, Hercules, CA). Chemiluminescent signal was recorded on a Fuji LAS-3000 imaging system (Tokyo, Japan) and quantified with ImageJ (<http://rsbweb.nih.gov/ij/>). For half-life experiments, a chase with 500 μ g/ml cycloheximide was performed as previously described (Hampton and Rine, 1994), and the value for Rpb1 in wild-type was calculated by linear regression of the logarithmized relative intensities.

ACCESSION NUMBERS

The cryo-EM structure of the Pol II-Iwr1 complex has been deposited at the EMDB (<http://www.ebi.ac.uk/pdbe/emdb/>) under the accession code EMD-1883. Raw and normalized transcriptional profiling data are available at ArrayExpress under the accession number E-MEXP-3126.

SUPPLEMENTAL INFORMATION

Supplemental Information includes Supplemental Experimental Procedures, Supplemental References, two figures, and two tables and can be found with this article online at doi:10.1016/j.molcel.2011.02.033.

ACKNOWLEDGMENTS

We thank A. Cook, C. Jung, A. Tresch, and members of the Cramer laboratory, in particular S. Benkert, A. Kusser, E. Lehmann, T. Koschubs, S. Sainsbury, and K. Maier. E.C. was supported by the Fonds der Chemischen Industrie. M.S. was supported by the Boehringer Ingelheim Fonds and the Elitenetzwerk Bayern. P.C. was supported by the Deutsche Forschungsgemeinschaft, the SFB646, TR5, FOR1068, the Nanosystems Initiative Munich (NIM), Bioimaging Network (BIN), and the Jung-Stiftung. Cryo-EM data were collected at the UltraStructure Network (USN), supported by the European Union and Senatsverwaltung für Wissenschaft, Forschung und Kultur Berlin.

Received: November 17, 2010

Revised: February 3, 2011

Accepted: February 24, 2011

Published: April 21, 2011

REFERENCES

Albuquerque, C.P., Smolka, M.B., Payne, S.H., Bafna, V., Eng, J., and Zhou, H. (2008). A multidimensional chromatography technology for in-depth phosphoproteome analysis. *Mol. Cell. Proteomics* 7, 1389–1396.

- Bianchi, M.M., Ngo, S., Vandenbol, M., Sartori, G., Morlupi, A., Ricci, C., Stefani, S., Morlino, G.B., Hilger, F., Carignani, G., et al. (2001). Large-scale phenotypic analysis reveals identical contributions to cell functions of known and unknown yeast genes. *Yeast* 18, 1397–1412.
- Boulon, S., Pradet-Balade, B., Verheggen, C., Molle, D., Boireau, S., Georgieva, M., Azzag, K., Robert, M.-C., Ahmad, Y., Neel, H., et al. (2010). HSP90 and its R2TP/Prefoldin-like cochaperone are involved in the cytoplasmic assembly of RNA polymerase II. *Mol. Cell* 39, 912–924.
- Cook, A., Fernandez, E., Lindner, D., Ebert, J., Schlenstedt, G., and Conti, E. (2005). The structure of the nuclear export receptor Cse1 in its cytosolic state reveals a closed conformation incompatible with cargo binding. *Mol. Cell* 18, 355–367.
- Cramer, P., Bushnell, D.A., Fu, J., Gnat, A.L., Maier-Davis, B., Thompson, N.E., Burgess, R.R., Edwards, A.M., David, P.R., and Kornberg, R.D. (2000). Architecture of RNA polymerase II and implications for the transcription mechanism. *Science* 288, 640–649.
- Cramer, P., Bushnell, D.A., and Kornberg, R.D. (2001). Structural basis of transcription: RNA polymerase II at 2.8 angstrom resolution. *Science* 292, 1863–1876.
- Cramer, P., Armache, K.J., Baumli, S., Benkert, S., Brueckner, F., Buchen, C., Damsma, G.E., Dengl, S., Geiger, S.R., Jasiak, A.J., et al. (2008). Structure of eukaryotic RNA polymerases. *Annu Rev Biophys* 37, 337–352.
- Damsma, G.E., Alt, A., Brueckner, F., Carell, T., and Cramer, P. (2007). Mechanism of transcriptional stalling at cisplatin-damaged DNA. *Nat. Struct. Mol. Biol.* 14, 1127–1133.
- Forget, D., Lacombe, A.A., Cloutier, P., Al-Khoury, R., Bouchard, A., Lavallée-Adam, M., Faubert, D., Jeronimo, C., Blanchette, M., and Coulombe, B. (2010). The protein interaction network of the human transcription machinery reveals a role for the conserved GTPase RPAP4/GPN1 and microtubule assembly in nuclear import and biogenesis of RNA polymerase II. *Mol. Cell. Proteomics* 9, 2827–2839.
- Gavin, A.C., Bösch, M., Krause, R., Grandi, P., Marzioch, M., Bauer, A., Schultz, J., Rick, J.M., Michon, A.M., Cruciat, C.M., et al. (2002). Functional organization of the yeast proteome by systematic analysis of protein complexes. *Nature* 415, 141–147.
- Hampton, R.Y., and Rine, J. (1994). Regulated degradation of HMG-CoA reductase, an integral membrane protein of the endoplasmic reticulum, in yeast. *J. Cell Biol.* 125, 299–312.
- He, X.J., Hsu, Y.F., Zhu, S., Liu, H.L., Pontes, O., Zhu, J., Cui, X., Wang, C.S., and Zhu, J.K. (2009). A conserved transcriptional regulator is required for RNA-directed DNA methylation and plant development. *Genes Dev.* 23, 2717–2722.
- Hodges, J.L., Leslie, J.H., Mosammamaparast, N., Guo, Y., Shabanowitz, J., Hunt, D.F., and Pemberton, L.F. (2005). Nuclear import of TFIIB is mediated by Kap114p, a karyopherin with multiple cargo-binding domains. *Mol. Biol. Cell* 16, 3200–3210.
- Hu, Z., Killion, P.J., and Iyer, V.R. (2007). Genetic reconstruction of a functional transcriptional regulatory network. *Nat. Genet.* 39, 683–687.
- Kanno, T., Bucher, E., Daxinger, L., Huettel, B., Kreil, D.P., Breinig, F., Lind, M., Schmitt, M.J., Simon, S.A., Gurazada, S.G., et al. (2010). RNA-directed DNA methylation and plant development require an IWR1-type transcription factor. *EMBO Rep.* 11, 65–71.
- Kettenberger, H., Eisenführ, A., Brueckner, F., Theis, M., Famulok, M., and Cramer, P. (2006). Structure of an RNA polymerase II-RNA inhibitor complex elucidates transcription regulation by noncoding RNAs. *Nat. Struct. Mol. Biol.* 13, 44–48.
- Kimura, M., Ishiguro, A., and Ishihama, A. (1997). RNA polymerase II subunits 2, 3, and 11 form a core subassembly with DNA binding activity. *J. Biol. Chem.* 272, 25851–25855.
- Kimura, M., Sakurai, H., and Ishihama, A. (2001). Intracellular contents and assembly states of all 12 subunits of the RNA polymerase II in the fission yeast *Schizosaccharomyces pombe*. *Eur. J. Biochem.* 268, 612–619.
- Knop, M., Finger, A., Braun, T., Hellmuth, K., and Wolf, D.H. (1996). Der1, a novel protein specifically required for endoplasmic reticulum degradation in yeast. *EMBO J.* 15, 753–763.
- Koschubs, T., Seizl, M., Larivière, L., Kurth, F., Baumli, S., Martin, D.E., and Cramer, P. (2009). Identification, structure, and functional requirement of the Mediator submodule Med7N/31. *EMBO J.* 28, 69–80.
- Kostrewa, D., Zeller, M.E., Armache, K.J., Seizl, M., Leike, K., Thomm, M., and Cramer, P. (2009). RNA polymerase II-TFIIB structure and mechanism of transcription initiation. *Nature* 462, 323–330.
- Kosugi, S., Hasebe, M., Tomita, M., and Yanagawa, H. (2009). Systematic identification of cell cycle-dependent yeast nucleocytoplasmic shuttling proteins by prediction of composite motifs. *Proc. Natl. Acad. Sci. USA* 106, 10171–10176.
- Krogan, N.J., Cagney, G., Yu, H., Zhong, G., Guo, X., Ignatchenko, A., Li, J., Pu, S., Datta, N., Tikuisis, A.P., et al. (2006). Global landscape of protein complexes in the yeast *Saccharomyces cerevisiae*. *Nature* 440, 637–643.
- Larivière, L., Seizl, M., van Wageningen, S., Röther, S., van de Pasch, L., Feldmann, H., Strässer, K., Hahn, S., Holstege, F.C., and Cramer, P. (2008). Structure-system correlation identifies a gene regulatory Mediator submodule. *Genes Dev.* 22, 872–877.
- Pagé, N., Gérard-Vincent, M., Ménard, P., Beaulieu, M., Azuma, M., Dijkgraaf, G.J., Li, H., Marcoux, J., Nguyen, T., Dowse, T., et al. (2003). A *Saccharomyces cerevisiae* genome-wide mutant screen for altered sensitivity to K1 killer toxin. *Genetics* 163, 875–894.
- Peiró-Chova, L., and Estruch, F. (2009). The yeast RNA polymerase II-associated factor Iwr1p is involved in the basal and regulated transcription of specific genes. *J. Biol. Chem.* 284, 28958–28967.
- Ranish, J.A., and Hahn, S. (1991). The yeast general transcription factor TFIIA is composed of two polypeptide subunits. *J. Biol. Chem.* 266, 19320–19327.
- Ream, T.S., Haag, J.R., Wierzbicki, A.T., Nicora, C.D., Norbeck, A.D., Zhu, J.K., Hagen, G., Guilfoyle, T.J., Pasa-Tolić, L., and Pikaard, C.S. (2009). Subunit compositions of the RNA-silencing enzymes Pol IV and Pol V reveal their origins as specialized forms of RNA polymerase II. *Mol. Cell* 33, 192–203.
- Reimand, J., Vaquerizas, J.M., Todd, A.E., Vilo, J., and Luscombe, N.M. (2010). Comprehensive reanalysis of transcription factor knockout expression data in *Saccharomyces cerevisiae* reveals many new targets. *Nucleic Acids Res.* 38, 4768–4777.
- Somesh, B.P., Reid, J., Liu, W.F., Søgaard, T.M., Erdjument-Bromage, H., Tempst, P., and Svejstrup, J.Q. (2005). Multiple mechanisms confining RNA polymerase II ubiquitylation to polymerases undergoing transcriptional arrest. *Cell* 121, 913–923.
- Somesh, B.P., Sigurdsson, S., Saeki, H., Erdjument-Bromage, H., Tempst, P., and Svejstrup, J.Q. (2007). Communication between distant sites in RNA polymerase II through ubiquitylation factors and the polymerase CTD. *Cell* 129, 57–68.
- Süel, K.E., and Chook, Y.M. (2009). Kap104p imports the PY-NLS-containing transcription factor Tfg2p into the nucleus. *J. Biol. Chem.* 284, 15416–15424.
- Sydow, J.F., Brueckner, F., Cheung, A.C., Damsma, G.E., Dengl, S., Lehmann, E., Vassilyev, D., and Cramer, P. (2009). Structural basis of transcription: mismatch-specific fidelity mechanisms and paused RNA polymerase II with frayed RNA. *Mol. Cell* 34, 710–721.
- Zhurinsky, J., Leonhard, K., Watt, S., Marguerat, S., Bähler, J., and Nurse, P. (2010). A coordinated global control over cellular transcription. *Curr. Biol.* 20, 2010–2015.